11

Short-term volume and turgor regulation in yeast

Jörg Schaber*[1] and Edda Klipp*†

**Max Planck Institute for Molecular Genetics, Computational Systems Biology, Ihnestr. 63–73, 14195 Berlin, Germany, and †Humboldt University Berlin, Institute for Biology, Theoretical Biophysics, Invalidenstr. 42, 10115 Berlin, Germany*

Abstract

Volume is a highly regulated property of cells, because it critically affects intracellular concentration. In the present chapter, we focus on the short-term volume regulation in yeast as a consequence of a shift in extracellular osmotic conditions. We review a basic thermodynamic framework to model volume and solute flows. In addition, we try to select a model for turgor, which is an important hydrodynamic property, especially in walled cells. Finally, we demonstrate the validity of the presented approach by fitting the dynamic model to a time course of volume change upon osmotic shock in yeast.

Introduction

In deterministic mathematical representations of biochemical reactions, molecule species usually communicate by their concentrations rather than by their molecule numbers. The reason for this is the observation that the rate of an elementary reaction, i.e. a reaction of only one state-transition, is, under certain conditions, proportional to the product of the concentrations of the participating molecules. In chemistry this is called the law of mass action, which is derived by statistical thermodynamics; concentration C is defined as the number of molecules N per volume V, such that $C = N/V$. Hence, it is

[1]*To whom correspondence should be addressed (email schaber@molgen.mpg.de).*

not surprising that cells highly regulate not only their molecule numbers by metabolism and protein production, but also their volume.

In the present chapter, we review basic principles of volume regulation and how it can be modelled mathematically. We concentrate on the volume regulation of cells upon a change in the osmotic conditions of the environment, henceforth called osmoregulation. We chose yeast cells because this system has been intensively studied and data are available.

Volume issues

One of the main features of osmoregulation in cells is volume change owing to flow of water and solutes across the cell membrane. Here we assume that, first, there is no volume change due to growth during osmoregulation and, secondly, that the volume change is only due to water flow and not to solute flows. Of course, solute flows are considered because they indirectly influence water flow by a change in water potential gradients. For the purpose of this study, we decompose the total cell volume V into the water volume, which is the osmotically active volume V_{os}, and the osmotically inactive or incompressible solid base volume V_b, that is assumed to be constant (eqn 1):

$$V = V_{os} + V_b \tag{1}$$

In the following, we will consider only one permeable solute, which, in the special case of yeast, will be glycerol.

Volume flow

The total volume change is assumed to be only due to water flow across the cell membrane dV_{os}/dt (in $\mu m^3/s$) driven by water and hydrodynamic potential gradients, which can be simplified to [1,2]:

$$\frac{dV}{dt} = \frac{d}{dt}\left(V_{os} + V_b\right) = \frac{dV_{os}}{dt} = L_p A(P - \Delta\Pi_n - \sigma\Delta\Pi_s)$$

where L_p is the hydraulic conductivity (in $\mu m \cdot MPa^{-1} \cdot s^{-1}$), A (in μm^2) is the cell surface area and P is the intracellular hydrostatic pressure exerted on the cell wall [turgor (in MPa)] that under steady-state conditions ($dV/dt = 0$) equilibrates $\Delta\Pi$. $\Delta\Pi$ is the osmotic pressure difference (in MPa) between the outside and the inside of the cell, where subscripts n and s denote non-permeable and permeable solutes in the following respectively, and σ is the dimensionless reflection coefficient [3]. As has been pointed out previously [2,3], when water and solutes are transported by different channels, which can be assumed to be the case in yeast with glycerol as the permeable solute, then

$$\sigma = 1 - \frac{k_s \overline{V}}{RTL_p}$$

where $\overline{V}$ is the partial molar volume of the solute, k_s (in $\mu m \cdot s^{-1}$) is the membrane solute permeability (see below), R is the gas constant (in $J \cdot mol^{-1} \cdot K^{-1}$) and T is the temperature (in K). In the case of glycerol ($\overline{V} \approx 0.071 \cdot 10^{-3} m^3/mol$) as the only solute at room temperature, σ approximates unity. Thus we assume (eqn 2):

$$\frac{dV_{os}}{dt} = L_p A(P - \Delta\Pi_{n+s}) \tag{2}$$

Depending on whether the effective water and solute exchange surface varies with volume, the cell surface can optionally be expressed as a function of volume as $A(t) = (36\pi)^{1/3} V(t)^{2/3}$ (in μm^2) assuming a spherical geometry of the cell. The osmotic pressure (in MPa) can be expressed according to van't Hoff's law [4] in terms of concentrations or molarities $\Delta\Pi = c_{PC} RT \Delta c$, where c is the concentration (in µM) and c_{PC} is a conversion factor relating pressure units to concentration units.

Thus eqn (2) becomes eqn (3):

$$\frac{dV_{os}}{dt} = L_p A(P - c_{PC} RT \Delta c) \tag{3}$$

with $\Delta c = c^e - c^i$, where superscripts e and i denote external and internal osmolytically active concentrations respectively. The external osmolarity can be written as $c^e = c_n^e + c_s^e$. Note that under turgid conditions $c^i > c^e$ and consequently $\Delta c < 0$. With this definition, under steady-state conditions the turgor $P < 0$.

If the system contains only one permeable solute (in our case glycerol) and if the total amount of the permeable and non-permeable solutes (in µmol) in the cell are denoted by N_s^i and N_n^i respectively, c^i becomes eqn (4):

$$c^i = \frac{N_s^i + N_n^i}{V_{os}} \tag{4}$$

It is convenient to also consider internal permeable and non-permeable solute concentrations, i.e. c_s^i and c_n^i (in $\mu mol \cdot \mu m^{-3}$) respectively. Eqn (4), with constant c_n^i, then becomes:

$$c^i = \frac{N_s^i + c_n^i V_{os,0}}{V_{os}} = c_s^i + c_n^i \frac{V_{os,0}}{V_{os}}$$

with $V_{os,0}$ as the initial osmotically active volume. Note that concentration changes in c_s^i due to volume change are considered separately in eqn (8).

We can then write eqn (3) as eqn (5):

$$\frac{dV_{os}}{dt} = L_p A\left(P - c_{PC} RT\left(c_s^e + c_n^e - c_s^i - c_n^i \frac{V_{os,0}}{V_{os}}\right)\right) \tag{5}$$

Assuming that eqn (5) is initially at steady state, i.e. $\frac{dV_{os}}{dt} = 0$ and $V_{os} = V_{os,0}$, then (eqn 6):

$$0 = \Delta P - c_{PC} RT \left(c^e_{s,0} + c^e_{n,0} - c^i_{s,0} - c^i_{n,0} \right) \tag{6}$$

At steady state we can furthermore assume $c^e_{s,0} = c^i_{s,0}$, such that we can estimate c^i_n from eqn (6) as a function of the initial turgor P_0 and the initial non-permeable external osmolarity $c^e_{n,0}$. Thus (eqn 7):

$$c^i_{n,0} = c^e_{n,0} - \frac{P_0}{c_{PC} RT} \tag{7}$$

Solute flow

The passive solute flow dN^i_s / dt (in μmol/s) across the membrane is calculated according to Fick's law as:

$$\frac{dN^i_s}{dt} = 10^{-15} \omega A R T (c^e_s - c^i_s)$$

where ω is the solute mobility per unit area (in $\mu mol \cdot s^{-1} \cdot Pa^{-1} \cdot m^{-2}$). Usually ωRT is identified with k_s (in $\mu m \cdot s^{-1}$) at constant temperature and can be regarded as the membrane solute permeability including the thickness of the membrane. As mentioned above, it is more convenient to consider solute concentrations. The change in intracellular permeable solutes (in $\mu mol \cdot \mu m^{-3} \cdot s^{-1}$) owing to production v_p, degradation v_d and regulated transport can be expressed as eqn (8):

$$\frac{dc^i_s}{dt} = v_p - v_d + p_{tr} k_s A \frac{(c^e_s - c^i_s)}{V_{os}} - \frac{c^i_s}{V_{os}} \frac{dV_{os}}{dt} \tag{8}$$

where p_{tr} is an additional parameter that can be viewed as a placeholder for a function to regulate the passive transport (see below). Assuming the change in external solute concentrations is influenced by outflow of intracellular solute, then (eqn 9) is:

$$\frac{dc^e_s}{dt} = -p_{tr} k_s A \frac{(c^e_s - c^i_s)}{V_{ex}} \tag{9}$$

where V_{ex} is the external volume (in μm^3) that we assume to be constant of a factor 1000 larger than the initial cell volume. Eqns (8) and (9) are also obtained when passive molecule transport across the cell boundary is modelled according to a mass action mechanism (eqn 10), i.e.

$$\frac{dc^e_s}{dt} = \frac{(v_{in} - v_{out})}{V_{ex}} \tag{10}$$

where v_{in} and v_{out} are the inward and outward molecule fluxes (in $\mu mol \cdot s^{-1}$) respectively, depending on the respective intra- and extracellular

concentrations (eqn 11):

$$\begin{aligned} v_{in} &= kc_i \\ v_{out} &= kc_e \end{aligned} \tag{11}$$

In this case, k (in $\mu m^3 \cdot s^{-1}$) is equal for both fluxes because both fluxes are mediated by the same channel. Setting $k = k_s A$ and inserting eqn (11) into eqn (10) we again arrive at eqn (9).

Eqn (10) has the advantage that different formulas for different transport mechanisms can be derived: assuming that the capacity of the channel(s) is limited, the molecule flux can be modelled according to eqn (12):

$$\begin{aligned} v_{in} &= \frac{kc_i}{K_m + c_i} \\ v_{out} &= \frac{kc_e}{K_m + c_e} \end{aligned} \tag{12}$$

Inserting eqn (12) into eqn (10) and setting $k = k_c A$, we arrive at:

$$\frac{dc_s^e}{dt} = -\frac{k_c A}{V_{ex}} \left(\frac{c_s^i}{K_m + c_s^i} - \frac{c_s^e}{K_m + c_s^e} \right)$$

with k_c (in $\mu mol \cdot \mu m^{-2} \cdot s^{-1}$). Note that at steady state we have equilibrated concentrations, i.e.

$$\frac{dc_s^e}{dt} = 0 \Leftrightarrow c_s^e = c_s^i$$

Turgor models

All cells maintain a water potential gradient across the membrane that is balanced by a hydrostatic pressure gradient, called turgor [5]. In walled cells, such as in plants and fungi, the turgor is usually much higher than in non-walled cells, because of the rigidity of the cell wall. In plants, the turgor adds to its mechanical stability and, both in plant and fungi, turgor is believed to play a role in cell growth [5]. From the notion that the cell wall is elastic, a decrease in turgor can be related to a fractional increase in volume independent of growth processes. This leads to the linear-elastic theory of turgor pressure (eqn 13):

$$dP = -\varepsilon \frac{dV}{V} \tag{13}$$

where ε is the elastic or Young's modulus (in MPa). Interpreting turgor as a function of volume, we can integrate eqn (13) using the substitution rule,

$$\int_{V_0}^{V} dP(V) = -\int_{V_0}^{V} \varepsilon \frac{1}{V} dV \quad \text{for } V \geq V_0$$

$$\Leftrightarrow P(V) - P(V_0) = -\varepsilon \ln\left(\frac{V}{V_0}\right)$$

Defining V_0 as the volume where the turgor becomes zero, i.e. $V_0 = V(P=0)$, $P(V_0)=0$ we arrive at an expression for the turgor as a function of volume (eqn 14),

$$P(V, V_0, \varepsilon) = -\varepsilon \ln\left(\frac{V}{V_0}\right) \text{ for } V \geq V_0 \tag{14}$$

and making a linear approximation (eqn 15):

$$P(V, V_0, \varepsilon) = \varepsilon\left(1 - \frac{V}{V_0}\right) \text{ for } V \geq V_0 \tag{15}$$

Now, there exist several possibilities as to what happens for $V < V_0$. Many models assume that below V_0 turgor is negligible [6,7]. One could also assume that the cell actually resists further compression below V_0, meaning that the turgor becomes positive. This could also be modelled as a linear elastic model, leading to (eqn 16):

$$P(V, V_0, \varepsilon_1, \varepsilon_2) = \begin{cases} \varepsilon_1\left(1 - \frac{V}{V_0}\right) & \textit{for } V \geq V_0 \\ \varepsilon_2\left(1 - \frac{V}{V_0}\right) & \textit{for } V < V_0 \end{cases} \tag{16}$$

In other publications [8,9] turgor is also modelled as a linear function of volume (eqn 17):

$$P(V, V_i, V_0, P_0) = -P_0\left(1 - \frac{V_i - V}{V_i - V_0}\right) \tag{17}$$

where P_0 and V_i are initial turgor and turgid volume respectively.

In contrast with eqn (17), eqns (14), (15) and (16) can predict the non-turgid volume V_0 given P_0 and V_i as $V_0 = V_i \exp^{\frac{P_0}{\varepsilon}}$ and, linearly approximated, $V_0 = \frac{\varepsilon V_i}{\varepsilon - P_0}$ respectively.

In Figure 1 we plot the turgor according to the three models (eqns 14–17) as a function of relative volume ($V_i = 100\%$) with values mostly from the literature.

Note that with the parameter from the literature, V_0 in eqns (14) and (15) was calculated as 99.3%, whereas in [8] V_0 was set to 63%. The linear approximation seems to be acceptable.

Selecting a turgor pressure model for yeast

Upon hyperosmotic shock, yeast cells rapidly shrink owing to a passive loss of water until a minimal volume is attained, where the external and internal osmotic pressures equilibrate. After this point, which we call the plasmolytic point, the cell produces osmotically active substances to increase the internal osmotic pressure and thereby forces water to flow back into the cell again, which results in a re-swelling [6,8,11–13] (Figure 3). Usually water has a much higher permeability compared with other permeable compounds. Thus we

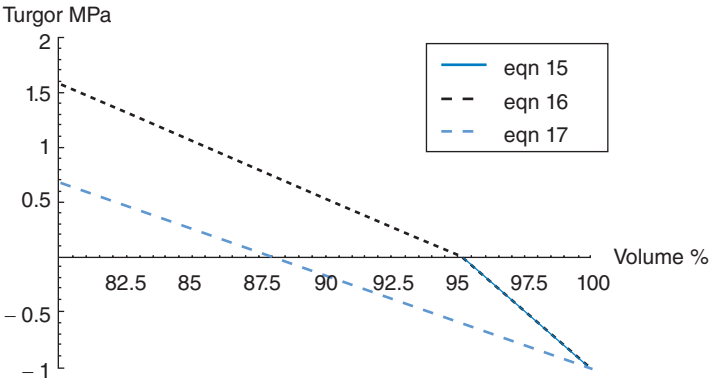

Figure 1. Turgor as a function of relative volume according to eqns (15–17)
$V_i = 100\%$, eqns (15) and (16): $\varepsilon_1 = 20$, $\varepsilon_2 = 10$, $P_0 = 1$, $V_0 = 95.1$; Eqn (17): $P_0 = -0.8$ [8], $V_0 = 88$ [8]. For eqns (15) and (16) only the linear approximations are displayed. The differences to the logarithmic form are negligible.

can assume that, at the plasmolytic point, no flow of soluble compounds has occurred yet, such that:

$$c^i_{s,0} + c^i_{n,0} = c^i_0$$

Moreover, at the plasmolytic point (eqn 18):

$$\begin{aligned} &\frac{dV_{os}}{dt} = 0 \\ \Leftrightarrow\ &0 = P_p - c_{PC}RT\left(c^e_n + c^e_0 - c^i_0\frac{V_{os,0}}{V_{os,\min}}\right) \\ \Leftrightarrow\ &0 = P_p - c_{PC}RT\left(c^e_n + c^e_0 - c^i_0\frac{V_i - V_b}{V_{\min} - V_b}\right) \end{aligned} \tag{18}$$

where P_p is the turgor at the plasmolytic point attained after an osmotic shock of c^e_n, according to one of the models (eqns 14–17); $V_{\mathrm{os,min}}$ and $V_{\min}$ are the attained minimal osmotically active and total volumes respectively; and c^i_0 and c^e_0 are the initial internal and external osmotically active solute concentrations, including permeable and non-permeable concentrations. Assuming an initial steady state, we can calculate c^i_0 from eqn (5), according to eqn (7), as (eqn 19):

$$c^i_0 = c^e_0 - \frac{P_0}{c_{PC}RT} \tag{19}$$

Thus, we can express $V_{\min}$ as a function of P_0, V_b and $\varepsilon_{1,2}$ or V_0, depending on the turgor model, and assuming that V_i, c^e_n and c^e_0 are known or at least measurable. For the non-linear model (eqn 14) we have to solve eqn (18) numerically, whereas for the linear models (eqns 15 and 17) we can derive an

analytical expression for $V_{\min}$. For eqn (15) this evaluates to, e.g.

$$0 = \varepsilon\left(1 - \frac{V_{\min}}{V_0}\right) - c_{PC}RT\left(c_n^e + c_0^e - c_0^i\frac{V_i - V_b}{V_{\min} - V_b}\right)$$

$$\Leftrightarrow V_{\min} = \frac{\varepsilon(V_b + V_0) + c_{PC}RTV_0\left(c_0^e - c_n^e\right)}{2\varepsilon} + \frac{\sqrt{4\varepsilon V_0\left(\varepsilon V_b - c_{PC}RTV_0\left(\left(c_n^e + c_0^e - c_0^i\right)V_b + c_0^i V_i\right)\right) + \left(c_{PC}RTV_0\left(c_n^e + c_0^e\right) - \varepsilon(V_b + V_0)\right)^2}}{2\varepsilon}$$

We can fit the different models to data by, e.g. minimizing the SSR (sum of squared residuals) between the calculated and measured minimal volume, i.e. $V_{\min}$ and V_{meas} respectively:

$$SSR(P_0, V_b, \varepsilon \textbf{ or } \varepsilon_{1,2} \textbf{ or } V_0) = \sum_{i=1}^{n}\left(V_{\min,i} - V_{meas,i}\right)^2$$

where n is the number of data points. We have used data from [6], where yeast cells were subjected to different concentrations of glycerol. We set the non-stressed volume to 100% at $c_0^e = 0.86$ M, which corresponds to an external osmotic pressure of 1.39 MPa (52 g of glycerol at T=25 °C, 1.39 MPa per litre of medium) in addition to the osmolarity of the medium, which is assumed to have an osmotically active concentration of 0.3 M according to our own measurements of YPD [1% (w/v) yeast extract/2% (w/v) peptone/2% (w/v) glucose]. For details concerning the measurements, please refer to [6].

The resulting SSR and estimated parameters are listed in Table 1.

In Figure 2, we display the best- and the worst-fit curves.

The simplest non-linear model (eqn 14), which assumes that the turgor becomes negligible below the non-turgid volume V_0, performs best. The

Table 1. Best fits and their respective parameters of the turgor models

The parameters for the different turgor models are displayed in the columns. The models are indicated by their type (lin. for linear and log. for logarithmic) and their formula number in the text respectively. p is the number of parameters of the respective SSR function. *Derived value.

Parameter	log. (eqn 14)	lin. (eqn 15)	log. (eqn 16)	lin. (eqn 16)	lin. (eqn 17)
SSR	14.25	14.26	15.1	14.3	20.5
p	3	3	4	4	3
V_0	89.8*	89.8*	90.2*	89.7*	95.2
V_b	59.1	59.2	59.6	59.5	60.4
ε1	20.3	19.3	21.3	18.9	
ε2			0.47	0.01	
P_0	–2.18	–2.18	–2.1	–2.2	–1.0

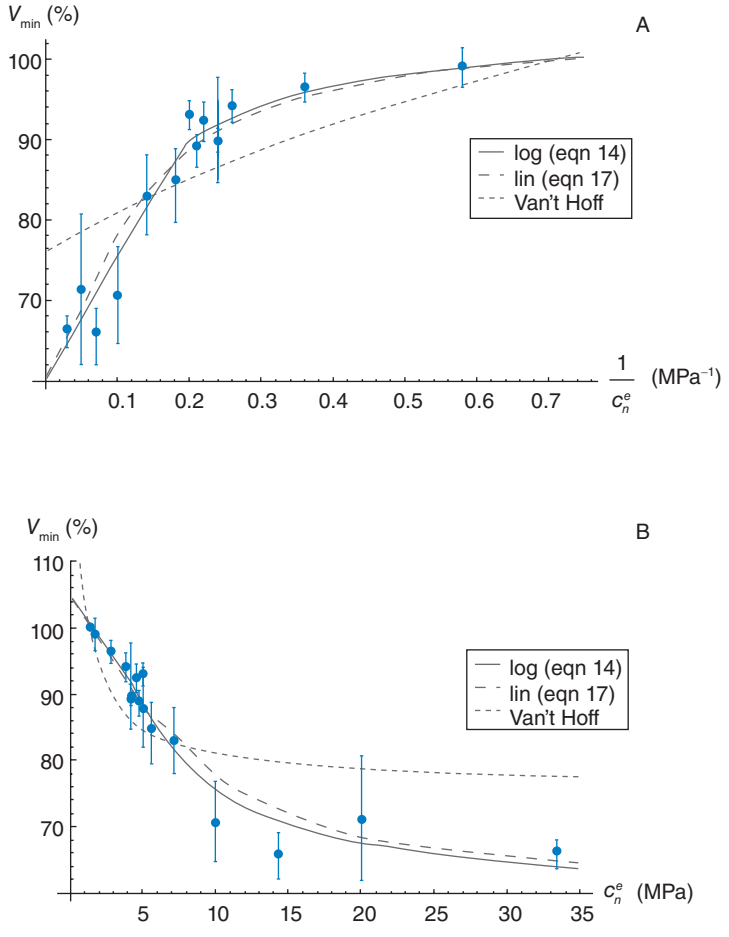

Figure 2. Data and fitted values for V_{min} of the three-parameter logarithmic models (eqns 14) (solid line) and the three-parameter linear model (eqn 17) (broken line) and according to van't Hoff's law (eqn 20) (dotted line)

(**A**) V_{min} against inverse applied external glycerol concentration in MPa^{-1}. (**B**) V_{min} against applied external glycerol concentration in MPa.

differences between the models are small. In Figure 2(A), V_{min} is displayed against the inverse of the applied osmotic stress. This representation is often used to support the assumption that, when the turgor is neglected, V_{min} is a linear function of the inverse applied osmotic stress. This also follows directly from van't Hoff's law and eqn (18) when $P_p = 0$ (eqn 20):

$$\begin{aligned} &\frac{dV_{os}}{dt} = 0 \\ \Leftrightarrow\ &0 = -c_{PC}RT\left(c_n^e + c_0^e - c_0^i\frac{V_{os,0}}{V_{os,\min}}\right) \\ \Leftrightarrow\ &V_{\min} = V_b + \frac{c_0^i(V_i - V_b)}{c_n^e + c_0^e} \end{aligned} \tag{20}$$

However, the model that assumes no turgor at all and calculates the minimal volume according to van't Hoff's law (eqn 20) is obviously not suitable (Figure 2, dotted curve). Interestingly, the fitted values only partially correspond to other measurements. Whereas the solid volume V_b (eqn 1) agrees with measurements [11], the elasticity ε and the initial turgor do not. Elasticity was estimated by compression experiments to be approx. 112 MPa [10] and estimation for the turgor varies between 0 and 1 MPa [14–17]. It is not clear whether these discrepancies are due to differences in yeast strains, experimental conditions or models. For the model fits we only considered c_0^i. However, as c_0^i is composed of permeable and non-permeable compounds, what can we say about their relationship? Assuming the one is a fraction f of c_0^i, $c_{s,0}^i = f c_0^i$, and under some steady-state assumption as in eqns (6) and (7) we can write:

$$c_{n,0}^e = c_0^e - c_{s,0}^e = c_0^e - c_{s,0}^i = c_0^e - f c_0^i = c_0^e - f\left(c_0^e - \frac{P_0}{c_{PC}RT}\right) > 0$$

$$\Leftrightarrow f < \frac{c_0^e}{c_0^e - \frac{P_0}{c_{PC}RT}}$$

Thus, given an initial external osmolarity, a fitted initial turgor and some initial steady-state assumption, we can derive a maximal fraction of internal permeable compounds. With the above assumptions on initial external osmolarity and the fitted turgor pressure of eqn (14) of 2.13 MPa $f \approx 0.5$, such that, at most, half of the initial intracellular osmolarity can be composed of permeable solutes. With the standard osmolarity of YPD of 0.3 M and the same turgor $f \approx 0.25$.

Volume dynamics

Eqns (5), (8) and (9), together with a model for turgor, constitute a complete system to model dynamic osmoregulation in yeast and, in fact, they have been used as a backbone for sophisticated models of osmoregulation [8,9]. In the following, we will use turgor model eqn (14). Upon osmotic shock, yeast cells produce glycerol as an osmolyte in order to equilibrate the osmotic pressure difference across the membrane and to force water back into the cell [11,12]. Another immediate response of yeast is the closure of the channel for glycerol, a protein called Fps1, such that the produced glycerol can be accumulated [18,19]. These two important processes can be modelled in a fairly simple way in order to explain measured data.

First, the production v_p in eqn (8) is modelled as a constant a, which is triggered by a change in turgor:

$$v_p = \begin{cases} a \text{ for } P > P_0 \\ 0 \text{ otherwise} \end{cases}$$

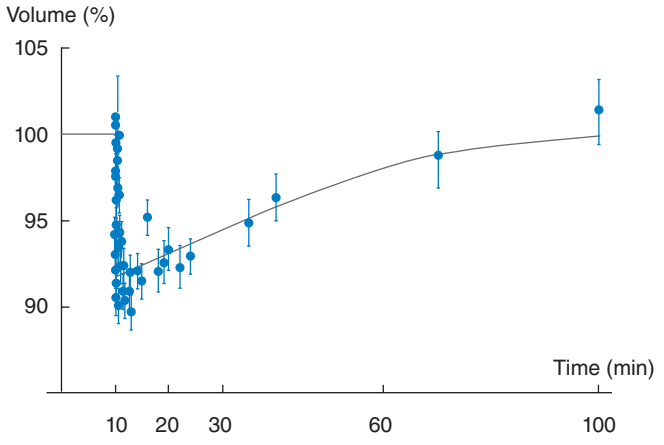

Figure 3. The data points represent measured volumes of yeast cells scaled to the initial size

The data are reproduced from [6] and correspond to a final water potential of 4.2 MPa. For details about the data see [6]. The solid lines are simulated time curves from the model described in the text. Model parameters: $L_p = 6.9 \times 10^{-4}$ μm·MPa^{-1}·s^{-1}, $k_s = 2.3 \times 10^{-4}$ μm·s^{-1}, $a = 0.01$ μM·s^{-1}, $c_0^e = 0.86$ M. The stress is induced after 10 min. The parameters for the turgor model are given in Table 1 (log of eqn 14).

Secondly, the transport of glycerol outside of the cell is also modulated by the turgor in a linear fashion:

$$p_{tr} = \begin{cases} 1 & \textit{for } P \le P_0 \\ P/P_0 & \textit{for } P_0 < P < 0 \\ 0 & \textit{otherwise} \end{cases}$$

Using the already fitted parameter from turgor model eqn (14) (Table 1), we only need to determine L_p, k_s and a to have a fully specified model. Initial concentrations were set and derived as above assuming that $c^i_{s,0} = c^i_{n,0}$ and $c^e_{s,0} = c^i_{s,0}$. We fit the parameters as described above to data from [6]. The results are displayed in Figure 3.

Obviously, the model is able to describe observed volume dynamics of yeast upon osmotic shock.

Conclusion

Basic thermodynamic considerations in conjunction with a model for turgor pressure and simple assumptions about the physiological processes, such as glycerol production and glycerol channel closure, are sufficient to explain the observed dynamics of volume changes of yeast cells upon external osmotic shock. The turgor pressure can be neglected when the volume falls below a certain threshold. Reports about the rigidity of the cell wall of yeast cells vary considerably.

Summary

- *Dynamics of volume change of yeast cells upon external osmotic shock can be simulated using basic thermodynamic and physiological models.*
- *A simple turgor model based on linear elastic theory fits the data well.*
- *Turgor can be neglected when the volume falls below a certain threshold.*

We thank Patrick Gervais for sending us a digital version of the data published in [6] that were used for the model fits. We also thank Clemens Kühn for measuring the osmolarity of YPD. E.K. is supported by the Max Planck Society and through funds of the European Commission (Integrated project BaSysBio, Network of Excellence ENFIN and the Yeast Systems Biology Network). J.S. is supported by the European Commission (contract number 043310).

References

1. Griffin, D.M. (1981) Water and microbial stress. *Adv. Microb. Ecol.* **5**, 91–136
2. Kleinhans, F.W. (1998) Membrane permeability modeling: Kedem–Katchalsky vs a two-parameter formalism. *Cryobiology* **37**, 271–289
3. Kedem, O. & Katchalsky, A. (1958) Thermodynamic analysis of the permeability of biological membranes to non-electrolytes. *Biochem. Biophys. Acta* **27**, 229–246
4. Noble, P.S. (1960) The Boyle–Van't Hoff relation. *J. Theor. Biol.* **23**, 375–379
5. Burström, H.G. (1971) Wishful thinking of turgor. *Nature* **234**, 488
6. Marechal, P.A., deMaranon, I.M., Molin, P. & Gervais, P. (1995) Yeast cell responses to water potential variations. *Int. J. Food Microbiol.* **28**, 277–287
7. Gervais, P., Molin, P., Marechal, P.A. & Herail-Foussereau, C. (1996) Thermodynamics of yeast cell osmoregulation: passive mechanisms. *J. Biol. Phys.* **22**, 73–86
8. Klipp, E., Nordlander, B., Kruger, R., Gennemark, P. & Hohmann, S. (2005) Integrative model of the response of yeast to osmotic shock. *Nat. Biotechnol.* **23**, 975–982
9. Gennemark, P., Nordlander, B., Hohmann, S. & Wedelin, D. (2006) A simple mathematical model of adaptation to high osmolarity in yeast. *In Silico Biol.* **6**, 193–214
10. Smith, A.E., Zhang, Z.B., Thomas, C.R., Moxham, K.E. & Middelberg, A.P.J. (2000) The mechanical properties of *Saccharomyces cerevisiae*. *Proc. Natl. Acad. Sci. U.S.A.* **97**, 9871–9874
11. Reed, R.H., Chudek, J.A., Foster, R. & Gadd, G.M. (1987) Osmotic significance of glycerol accumulation in exponentially growing yeasts. *Appl. Environ. Microbiol.* **53**, 2119–2123
12. Hohmann, S. (2002) Osmotic adaptation in yeast: control of the yeast osmolyte system. *Int. Rev. Cytol.* **215**, 149–187
13. Eriksson, E., Enger, J., Nordlander, B., Erjavec, N., Ramser, K., Goksor, M., Hohmann, S., Nystrom, T. & Hanstorp, D. (2007) A microfluidic system in combination with optical tweezers for analyzing rapid and reversible cytological alterations in single cells upon environmental changes. *Lab. Chip* **7**, 71–76
14. Marechal, P.A. & Gervais, P. (1994) Yeast viability related to water potential variation: influence of the transient phase. *Appl. Microbiol. Biotechnol.* **42**, 617–622
15. Gervais, P., Molin, P., Marechal, P.A. & HerailFoussereau, C. (1996) Thermodynamics of yeast cell osmoregulation: passive mechanisms. *J. Biol. Phys.* **22**, 73–86
16. Martinez de Maranon, I., Marechal, P.A. & Gervais, P. (1996) Passive response of *Saccharomyces cerevisiae* to osmotic shifts: cell volume variations depending on the physiological state. *Biochem. Biophys. Res. Commun.* **227**, 519–523

17. Smith, A.E., Zhang, Z. & Thomas, C.R. (2000) Wall material properties of yeast cells: part 1. Cell measurements and compression experiments. *Chem. Eng. Sci.* **55**, 2031–2041
18. Karlgren, S., Filipsson, C., Mullins, J.G., Bill, R.M., Tamas, M.J. & Hohmann, S. (2004) Identification of residues controlling transport through the yeast aquaglyceroporin Fps1 using a genetic screen. *Eur. J. Biochem.* **271**, 771–779
19. Karlgren, S., Pettersson, N., Nordlander, B., Mathai, J.C., Brodsky, J.L., Zeidel, M.L., Bill, R.M. & Hohmann, S. (2005) Conditional osmotic stress in yeast: a system to study transport through aquaglyceroporins and osmostress signaling. *J. Biol. Chem.* **280**, 7186–7193